AGU PUBLICATIONS

Water Resources Research

RESEARCH ARTICLE
10.1002/2013WR015112

Key Points:
- Hydrologic variability is a major control of invertebrate habitat suitability
- New analytical basin-scale approach for pdfs of ecohydrological key features
- Austrian river basin used for ecohydrological data-model comparison

Supporting Information:
- Readme
- Figure S1

Correspondence to:
S. Ceola,
serena.ceola@unibo.it

Citation:
Ceola, S., E. Bertuzzo, G. Singer, T. J. Battin, A. Montanari, and A. Rinaldo (2014), Hydrologic controls on basin-scale distribution of benthic invertebrates, *Water Resour. Res.*, *50*, 2903–2920, doi:10.1002/2013WR015112.

Received 27 NOV 2013
Accepted 11 MAR 2014
Accepted article online 15 MAR 2014
Published online 2 APR 2014

Hydrologic controls on basin-scale distribution of benthic invertebrates

Serena Ceola[1], Enrico Bertuzzo[2], Gabriel Singer[3,4], Tom J. Battin[3,5], Alberto Montanari[1], and Andrea Rinaldo[2,6]

[1]Department DICAM, University of Bologna, Bologna, Italy, [2]Laboratory of Ecohydrology, School of Architecture, Civil and Environmental Engineering, École Polytechnique Fédérale de Lausanne, Lausanne, Switzerland, [3]Department of Limnology and Oceanography, University of Vienna, Vienna, Austria, [4]Department of Ecohydrology, Leibniz-Institute for Freshwater Ecology and Inland Fisheries, Berlin, Germany, [5]WasserCluster Lunz, Interuniversitary Center for Aquatic Ecosystem Research, Lunz am See, Austria, [6]Dipartimento di Ingegneria Civile, Edile ed Ambientale, Università di Padova, Padova, Italy

Abstract Streamflow variability is a major determinant of basin-scale distributions of benthic invertebrates. Here we present a novel procedure based on a probabilistic approach aiming at a spatially explicit quantitative assessment of benthic invertebrate abundance as derived from near-bed flow variability. Although the proposed approach neglects ecological determinants other than hydraulic ones, it is nevertheless relevant in view of its implications on the predictability of basin-scale patterns of organisms. In the present context, aquatic invertebrates are considered, given that they are widely employed as sensitive indicators of fluvial ecosystem health and human-induced perturbations. Moving from the analytical characterization of site-specific probability distribution functions of streamflow and bottom shear stress, we achieve a spatial extension to an entire stream network. Bottom shear stress distributions, coupled with habitat suitability curves derived from field studies, are used to produce maps of invertebrate suitability to shear stress conditions. Therefore, the proposed framework allows one to inspect the possible impacts on river ecology of human-induced perturbations of streamflow variability. We apply this framework to an Austrian river network for which rainfall and streamflow time series, river network hydraulic properties, and local information on invertebrate abundance for a limited number of sites are available. A comparison between observed species density versus modeled suitability to shear stress is also presented. Although the proposed strategy focuses on a single controlling factor and thus represents an ecological minimal model, it allows derivation of important implications for water resource management and fluvial ecosystem protection.

1. Introduction

Predicting the effects of hydrologic fluctuations on ecological processes at the catchment scale of fluvial environments is a topical issue in ecohydrology [*Zalewski et al*., 1997; *Rodriguez-Iturbe*, 2000; *Rouget et al*., 2006; *Rodriguez-Iturbe et al*., 2009; *Szemis et al*., 2013; *Mejía et al*., 2014]. Geomorphology, hydrology, stream water chemistry, and temperature are all factors that control ecological processes in fluvial ecosystems [*Allan and Castillo*, 2007]. River discharge and the fluvial network structure are considered as major variables that affect population dynamics of benthic communities in stream and river ecosystems [*Poff and Ward*, 1989; *Hart and Finelli*, 1999; *Allan and Castillo*, 2007]. Accordingly, discharge and network structure are accounted for in both individual based and metacommunity models reproducing dynamics of ecological corridors [*Muneepeerakul et al*., 2008; *Rodriguez-Iturbe et al*., 2009].

River discharge is a complex outcome of forms and functions of a river basin, which integrates climate, land use, and geomorphological processes [e.g., *Leopold et al*., 1964; *Rodriguez-Iturbe and Rinaldo*, 1997]. Catchment heterogeneity and the time-variable rainfall patterns are reflected in the intrinsic stochasticity of streamflow, given each river a distinct physical fingerprint. A rigorous derivation of the probability distribution function (pdf) of streamflow as a function of underlying processes such as precipitation, evapotranspiration, runoff generation, and routing, has recently been provided by *Botter et al*. [2007a]. Spatiotemporal variability of streamflow implies spatiotemporal changes of associated hydraulic variables like flow velocity, water depth, bottom shear stress, and shear velocity, which influence and control benthic species

abundance and community structure in stream ecosystems [*Biggs et al*., 1990; *Hart and Finelli*, 1999]. In particular, shear stress is a major control on benthic life [*Statzner and Muller*, 1989; *Poff and Ward*, 1992; *Vogel*, 1994; *Malmqvist and Sackmann*, 1996; *Hart and Finelli*, 1999; *Gore et al*., 2001; *Lancaster et al*., 2006; *Trent and Ackerman*, 2011], for example, influencing the crawling behavior and foraging activities of benthic invertebrates [*Lancaster and Hildrew*, 1993; *Power et al*., 1995a; *Wellnitz et al*., 2001; *Lancaster et al*., 2006; *Ceola et al*., 2013]. A plethora of scientific contributions analyzed the relationship of benthic invertebrate species distribution and density with bottom shear stress from various field studies across the world [see, e.g., *Statzner and Muller*, 1989; *Schmedtje*, 1995; *Doledec et al*., 2007; *Merigoux et al*., 2009; *Lamouroux et al*., 2013; *Booker et al*., 2014]. Therefore, changes in streamflows, which translates into changes in near-bed hydraulic conditions, may be a potential explanatory variable to predict changes in benthic communities [*Gore et al*., 2001].

In addition, network structure and connectivity of the river basin prove fundamental in a variety of ecohydrological processes. From field studies to metacommunity models, the dendritic geometry of fluvial ecosystems has emerged as a major control on ecological processes and dynamics in these systems [see, e.g., *Fagan*, 2002; *Campbell Grant et al*., 2007; *Muneepeerakul et al*., 2007; *Battin et al*., 2008; *Muneepeerakul et al*., 2008; *Bertuzzo et al*., 2009, 2011; *Carrara et al*., 2012; *Besemer et al*., 2013]. The aforementioned controls of both river network structure and spatial and temporal variability of hydrologic variables on riverine ecological communities highlight relevant scientific questions related to the theoretical description of the interactions and feedbacks among hydrology, geomorphology, ecology, and anthropogenic activities.

We present a general and original analytical approach to describe the probability distribution of relevant hydrologic variables (streamflow and bottom shear stress) and associated habitat suitability for invertebrates along a river network. The novel spatially explicit procedure makes use of suitable geomorphological scaling relationships. The approach is applied—as an example—to a prealpine river basin located in Austria, for which data on rainfall, streamflow time series, and invertebrate abundance are available. Moving from the analytical characterization of the site-specific streamflow Q and bottom shear stress τ probability distributions [*Botter et al*., 2007a; *Ceola et al*., 2013], scaling relations defining geomorphic properties along the river network are used to derive the spatiotemporal distribution of Q and τ. To this aim, site-specific ecohydrological probability distribution functions are employed and extended to the examined river network. For a set of selected invertebrate species, we then use the leading hydrologic and geomorphologic probability distributions to derive probability distribution maps for habitat suitability, which essentially scales linearly to invertebrate abundance based on their tolerance to shear stress. Given that benthic invertebrates are sensitive indicators of fluvial ecosystems health, the proposed model is meant to provide support to environmental management studies related, for instance, to the definition of environmental flow requirements and habitat protection. Although the available data on species distribution allow a limited assessment of the validity of the proposed modeling framework, we present a comparison between analytical invertebrate suitability to near-bed flow conditions and measured species abundance. The analysis points toward the kind of data set needed to fully validate the model in future analyses.

2. Materials and Methods

2.1. Probabilistic Characterization of Site-Specific Flow Variables

The temporal variability of geometric and kinematic hydraulic variables in a considered cross section (i.e., streamflow Q, water depth d, flow velocity v, and average bottom shear stress τ) is mainly influenced by the rainfall forcing. Following *Botter et al*. [2007a, 2008], the probabilistic characterization of river streamflow Q [$L^3\,T^{-1}$] can be derived from a stochastic analysis of the dynamics of soil moisture, which controls the slow-subsurface component of runoff, coupled to the response function of the catchment (i.e., storage-discharge relationship). The analytical expression of the seasonal streamflow distribution (i.e., where a season consists of a 3 month period with constant rainfall statistics and geomorphological features) is based on the following modeling scheme assumptions we briefly recall here [*Botter et al*., 2007a]:

1. The main contribution to streamflow formation is given by subsurface runoff. Such an assumption is compatible with the case of catchments characterized by limited imperviousness when referring to extended time scales (daily or higher).

2. Rainfall events are modeled on a daily basis as a zero-dimensional Poisson process with average frequency λ_p [T^{-1}], whereas rainfall depths are assumed to follow an exponential distribution with mean α [L]

[*Rodriguez-Iturbe et al*., 1999; *Rodriguez-Iturbe and Porporato*, 2004]. These assumptions presume that (i) the spatial correlation scale of rainfall events is greater than the catchment size (i.e., uniform rainfall within the catchment), and (ii) the time scale of the process is greater than the characteristic duration of a rainfall event (i.e., daily time scale).

3. Soil moisture dynamics, which contributes to subsurface runoff, is governed by the fraction of rainfall which infiltrates into the surface soil layers (i.e., effective rainfall). Effective streamflow-producing rainfall events can be modeled at a daily time scale as a zero-dimensional Poisson process with average frequency $\lambda < \lambda_p$ [T^{-1}], while effective rainfall depths are exponentially distributed with the same mean of rainfall events α [L] [*Rodriguez-Iturbe et al*., 1999; *Rodriguez-Iturbe and Porporato*, 2004].

4. Effective rainfall contributing to runoff production is then released from the soil to the channel network following a linear storage-discharge relation [*Botter et al*., 2007a], which assumes a widely employed [see, e.g., *Chow et al*., 1988; *Beven*, 2001; *Brutsaert*, 2005] exponential response function, with mean response time $1/k$ [T].

The site-specific streamflow probability distribution function obtained from this modeling scheme is a gamma distribution [*Botter et al*., 2007a]:

$$p_Q(Q) = \frac{(\alpha k A)^{-1}}{\Gamma\left(\frac{\lambda}{k}\right)} \left(\frac{Q}{\alpha k A}\right)^{\frac{\lambda}{k}-1} e^{-\frac{Q}{\alpha k A}}, \tag{1}$$

where A [L^2] represents the catchment area and $\Gamma(\cdot)$ is the complete gamma function. The streamflow distribution given by equation (1) has been extensively applied to several catchments located in different climatic and geomorphological regions of the world and shows a remarkable capability of reproducing the observed streamflow dynamics [*Botter et al*., 2007b, 2008; *Ceola et al*., 2010].

Following *Ceola et al*. [2013], the site-specific probability distribution functions of relevant flow variables can be derived from the streamflow distribution using additional information on the geomorphic and hydraulic properties of the examined river cross section. Here we focus only on average bottom shear stress τ [$M\,L^{-1}\,T^{-2}$], which is considered a key control on the activity and spatial distribution of benthic biota [*Poff and Ward*, 1992; *Vogel*, 1994; *Malmqvist and Sackmann*, 1996; *Hart and Finelli*, 1999; *Trent and Ackerman*, 2011]. Extensions to water depth and flow velocity can be straightforwardly developed in the same manner. Assuming locally uniform flow conditions, cross-section averaged bottom shear stress is given by:

$$\tau = \rho g R_h s, \tag{2}$$

where ρ [$M\,L^{-3}$] is the water density, g [$L\,T^{-2}$] is the acceleration of gravity, R_h [L] is the hydraulic radius (i.e., the ratio of wetted area to wetted perimeter), and s [-] is the suitably averaged local slope. By employing a Manning-like uniform flow relation [e.g., *Chow*, 1964], and a scaling relation between the hydraulic radius and discharge downsizing that between landscape-forming discharge and channel width-depth ratio [*Leopold et al*., 1964], one obtains a suitable approximation involving a one-to-one relationship between streamflow Q and shear stress τ, expressed as a power-law equation of the type:

$$\tau = c_\tau Q^{e_\tau}, \tag{3}$$

where c_τ[$ML^{-3e_\tau-1}T^{e_\tau-2}$] depends on the hydraulic geometry and characteristics of the cross section (i.e., river width, bed slope, and roughness) and e_τ [-] is a constant exponent. By coupling equations (1) and (3), the analytical expression of the site-specific probability distribution function of average bottom shear stress can be obtained as a derived-distribution and reads as the following generalized gamma distribution [*Ceola et al*., 2013]:

$$p_\tau(\tau) = \frac{\theta_\tau}{e_\tau \Gamma\left(\frac{\lambda}{k}\right)} (\theta_\tau \tau)^{\frac{\lambda}{e_\tau k}-1} e^{-(\theta_\tau \tau)^{\frac{1}{e_\tau}}}, \tag{4}$$

where $\theta_\tau = \frac{(\alpha A k)^{-e_\tau}}{c_\tau}$ is proportional to the mean streamflow increment due to incoming effective rainfall events. c_τ can be estimated by assuming that (i) flow conditions are uniform, (ii) the river cross section

approximates a rectangular shape of area $S = wd$ [L^2], where w [L] and d [L] are river width and water depth, respectively, and (iii) the river width is much larger than the water depth (i.e., $w >> d$). Then the hydraulic radius can be expressed merely in terms of water depth and the bottom shear stress reads:

$$\tau \simeq \rho g d s. \tag{5}$$

By coupling equations (3) and (5), where the water depth d is derived from the continuity and the Manning's equations, one obtains:

$$c_\tau = \rho g s \left(\frac{1}{n} s^{1/2} w\right)^{-e_\tau}, \tag{6}$$

where n [$T L^{-1/3}$] is the Manning coefficient, related to bed surface roughness, and $e_\tau = 3/5$. Our main focus here is on cross-section averaged bottom shear stress, resulting from balancing gravity and resistance forces by assuming locally near-uniform and quasi-parallel flow. On a smaller spatial scale, local shear stress conditions, which may differ from the average value, might be recovered from local water depth and involving considerations on the active layer for sediment transport and the grain-size composition of the bottom material [see, e.g., *Armanini and Di Silvio*, 1988; *Armanini*, 1995]. We believe, however, that a basin-scale assessment of habitat suitability as given by shear stress adequately refers to an average site-specific shear stress (i.e., 1-D evaluation).

2.2. Basin-Scale Relations of River Network Geomorphic and Hydrologic Properties

The geomorphic characteristics of a river channel are determined by fluvial processes, and in particular by discharge and sediment properties, which vary along the river network [*Leopold et al*., 1964; *Orlandini and Rosso*, 1998]. It is well known that in the downstream direction, rivers usually increase in width, depth, and (significantly less) mean velocity, while they slightly decrease in bed roughness. From measured data, *Leopold et al*. [1964] provided analytical relationships describing the variability of selected geomorphic characteristics of a river channel in a downstream direction as a function of discharge, where either the mean annual or the bankfull discharge, characterized by a return period equal to 0.25 and 2 years, respectively, could be used as explanatory variables. The scaling relations for river width w, water depth d, flow velocity v, and bed roughness, expressed in terms of the Manning coefficient n, widely employed across various river systems throughout the world, read, respectively, as:

$$w = c_w Q^{e_w}, \tag{7}$$

$$d = c_d Q^{e_d}, \tag{8}$$

$$v = c_v Q^{e_v}, \tag{9}$$

$$n = c_n Q^{e_n}, \tag{10}$$

where $c_w[L^{1-3e_w}T^{e_w}]$, e_w[-], $c_d[L^{1-3e_d}T^{e_d}]$, e_d[-], $c_v[L^{1-3e_v}T^{e_v-1}]$, e_v [-], $c_n[L^{-1/3-3e_n}T^{e_n+1}]$, and e_n [-] are coefficients. From the continuity equation, one obtains that $c_w c_d c_v = 1$ and $e_w + e_d + e_v = 1$. From USGS gauging stations, *Leopold et al*. [1964] found $e_w = 0.5, e_d = 0.4, e_v = 0.1$, and $e_n = -0.2$. Alternative exponent values obtained from a larger data set [*Raymond et al*., 2012] read $e_w = 0.42, e_d = 0.29$, and $e_v = 0.28$. Analogously, *Leopold et al*. [1964] expressed the scaling relation between river bed slope s and discharge Q as $s = c_s Q^{e_s}$, where $c_s[L^{-3e_s}T^{e_s}]$ and e_s [-] are constants. In this case $e_s = -0.5$ and therefore the channel slope decreases with increasing discharge. By assuming uniform rainfall over the catchment (see section 2.1), Q is directly proportional to A and therefore these relations can be also expressed in terms of the drainage area A.

Concerning the mean response time of a catchment, a relation widely applied in hydrology assumes that k [T^{-1}] (i.e., the inverse of the catchment response time) varies with the drainage area following a power-law relation of the type $k = c_k A^{e_k}$ [*Robinson and Sivapalan*, 1997], where $c_k[L^{-2e_k}T^{-1}]$ and e_k [-] are scaling coefficients. In a directed network, the mean length of the hydraulic path from a given location i to the outlet is proportional to $A_i^{0.5}$ [*Banavar et al*., 1999]. Thus, assuming that the residence time is proportional to the path length, e_k is found equal to -0.5. Geomorphological distinctions between

channeled and unchanneled paths to the outlet suggest a scaling pattern as well [*Rinaldo et al.*, 1995]. In view of the above considerations and following *Pilgrim* [1987], *Rinaldo et al.* [1991] and *Robinson and Sivapalan* [1997], who regard the spatial uniformity of flow velocity as a trade-off of downstream decaying slope and flow resistance, the scaling exponent e_k is suggested to lie within the range from -0.6 to -0.3.

2.3. Spatially Explicit Probability Distributions of Hydrologic Variables

As discussed in section 2.2, the spatial distribution of the drainage area along a river network influences the spatial variability of discharge and associated hydraulic conditions. Here we perform a spatial extension to an entire river catchment to derive a spatially explicit probability distribution from the site-specific characterization of the probability distributions presented in section 2.1.

The streamflow gamma distribution (equation (1)) is characterized by three parameters, namely α and λ, which are assumed constant within the river catchment [*Botter et al.*, 2007a], and k, whose value changes along the river network, as already outlined in section 2.2. Each site along the river network is thus characterized by a discharge temporal sequence, $Q(t)$, whose magnitude is intimately associated with the contributing area of the considered river cross section. At any location along the river network, the streamflow temporal mean $\langle Q \rangle$, variance σ_Q^2, and coefficient of variation CV_Q can be evaluated as a function of the gamma distribution parameters as follows [*Botter et al.*, 2007a]:

$$\langle Q \rangle = \alpha A \lambda, \tag{11}$$

$$\sigma_Q^2 = (\alpha A)^2 \lambda k, \tag{12}$$

$$CV_Q = \frac{\sigma_Q}{\langle Q \rangle}, \tag{13}$$

where σ_Q is the streamflow standard deviation.

Analogously, a peculiar temporal sequence of $\tau(t)$ identifies each node of the river network for which the temporal mean $\langle \tau \rangle$, variance σ_τ^2, and coefficient of variation CV_τ can be evaluated as a function of the drainage area A, the coefficients c_τ and e_τ of equations (3) and (6) and the three parameters of the streamflow gamma distribution (equation (1)). In order to estimate $\langle \tau \rangle$, σ_τ^2, and CV_τ, the generalized gamma distribution (equation (4)), is characterized by the following expression for the rth order moments [*Stacy*, 1962; *Johnson et al.*, 1994]:

$$E(\tau^r) = \left(\frac{1}{\theta_\tau}\right)^r \frac{\Gamma\left[e_\tau\left(\frac{\lambda}{e_\tau k} + r\right)\right]}{\Gamma(\lambda/k)}, \tag{14}$$

where $r \geq 1$. Therefore, the shear stress temporal mean $\langle \tau \rangle$ is derived from equation (14) with $r = 1$ and reads:

$$\langle \tau \rangle = \left(\frac{1}{\theta_\tau}\right) \frac{\Gamma\left[e_\tau\left(\frac{\lambda}{e_\tau k} + 1\right)\right]}{\Gamma(\lambda/k)}. \tag{15}$$

The shear stress variance σ_τ^2 is defined as:

$$\sigma_\tau^2 = \langle \tau^2 \rangle - \langle \tau \rangle^2, \tag{16}$$

and by substituting equations (14) and (15) into (16) one obtains:

$$\sigma_\tau^2 = \left(\frac{1}{\theta_\tau}\right)^2 \frac{\Gamma\left[e_\tau\left(\frac{\lambda}{e_\tau k} + 2\right)\right]}{\Gamma(\lambda/k)} - \left[\left(\frac{1}{\theta_\tau}\right) \frac{\Gamma\left[e_\tau\left(\frac{\lambda}{e_\tau k} + 1\right)\right]}{\Gamma(\lambda/k)}\right]^2. \tag{17}$$

The coefficient of variation CV_τ is expressed as:

$$CV_\tau = \frac{\sigma_\tau}{\langle \tau \rangle}, \tag{18}$$

where σ_τ is the shear stress standard deviation. Equations (15), (17), and (18) apply also for water depth d and flow velocity v, with appropriate distribution parameters.

2.4. Spatially Explicit Invertebrate Habitat Suitability

Based on sections 2.1–2.3, we can provide basin-scale information on near-bed fluvial ecosystems, as outlined in what follows. Benthic habitats are notably influenced by the intrinsic heterogeneity of environmental conditions [*Ceola et al.*, 2013]. In particular, the near-bed hydraulic conditions, subsumed by the average bottom shear stress τ, constitute a major control on the spatial distribution and grazing activity of benthic invertebrates like mayflies (*Ephemeroptera*) [*Poff and Ward*, 1992; *Vogel*, 1994; *Malmqvist and Sackmann*, 1996; *Hart and Finelli*, 1999; *Doledec et al.*, 2007; *Merigoux et al.*, 2009; *Trent and Ackerman*, 2011; *Lamouroux et al.*, 2013]. Mayflies are characterized by a short adult stage [*Merritt and Cummins*, 1996] and they are often included as indicator species in stream biota surveys. To synthesize hydrologic controls one may use a habitat suitability curve [e.g., *Jowett and Richardson*, 1990; *Jowett et al.*, 1991], which describes the effects of any generic environmental variable on species behavior and distribution, and is a fundamental tool to describe species habitat preferences. *Statzner and Muller* [1989] and *Schmedtje* [1995] report independently validated relationships between bottom shear stress and suitability for benthic invertebrates from a prealpine study stream. Here we combine these relationships with the shear stress probability distribution function previously presented to derive a spatially distributed assessment of habitat suitability for selected species at the scale of an entire river network. Specifically, a power-law fit to habitat suitability field data [*Schmedtje*, 1995] is used to model the relation between habitat suitability and bottom shear stress, and to consequently characterize the probability distribution function of habitat suitabilities to shear stress as follows:

$$\psi = c_{\psi_\tau} \tau^{e_{\psi_\tau}}, \tag{19}$$

where ψ [-] identifies a measure of habitat suitability to shear stress, while $c_{\psi_\tau}[\mathrm{M}^{-e_{\psi_\tau}}\mathrm{L}^{e_{\psi_\tau}}\mathrm{T}^{2e_{\psi_\tau}}]$ and e_{ψ_τ}[-] are constants. By substituting equation (3) into (19), the habitat suitability ψ, expressed as a function of discharge, becomes:

$$\psi = c_\psi Q^{e_\psi}, \tag{20}$$

where $c_\psi = c_{\psi_\tau} c_\tau^{e_{\psi_\tau}}[\mathrm{L}^{-3e_\psi}\mathrm{T}^{e_\psi}]$ and $e_\psi = e_{\psi_\tau} e_\tau$[-]. Therefore, the site-specific analytical characterization of the probability distribution function of species habitat suitability to shear stress can be obtained as a derived-distribution from equation (1) and it is expressed by the following generalized gamma distribution:

$$p_\psi(\psi) = \frac{\theta_\psi}{e_\psi \Gamma\left(\frac{\lambda}{k}\right)} (\theta_\psi \psi)^{\frac{\lambda}{e_\psi k}-1} e^{-(\theta_\psi \psi)^{\frac{1}{e_\psi}}}, \tag{21}$$

where $\theta_\psi = \frac{(\alpha A k)^{-e_\psi}}{c_\psi}$ is a function of the geomorphic and hydrologic properties of the river network and of the ecological traits of the considered species. Figure 1 shows possible shapes of the analytical pdf of species habitat suitability (equation (21)), expressed in terms of species density, for different parameter combinations. Irrespective of whether a power-law relation between habitat suitability and shear stress applies, the developed method provides a tool to sort out the spatial distribution of a species' relative occurrence probability, by using numerical simulation to transfer the time series of τ into a time series of ψ. In analogy with the performed analyses for discharge and bottom shear stress, the species habitat suitability temporal mean $\langle \psi \rangle$, variance σ_ψ^2, and coefficient of variation CV_ψ, can be evaluated along a river network, where θ_ψ and e_ψ are substituted into equations (15), (17), and (18), thus providing relevant information about benthic conditions in streams and rivers.

3. Case Study

The analytical model described in section 2 is applied to the Ybbs catchment (Austria, 47.81°N, 14.94°E, Figure 2), where streamflow and rainfall time series, and river network hydraulic properties are available. Furthermore, snapshot information on the abundance of various mayfly species is available as well.

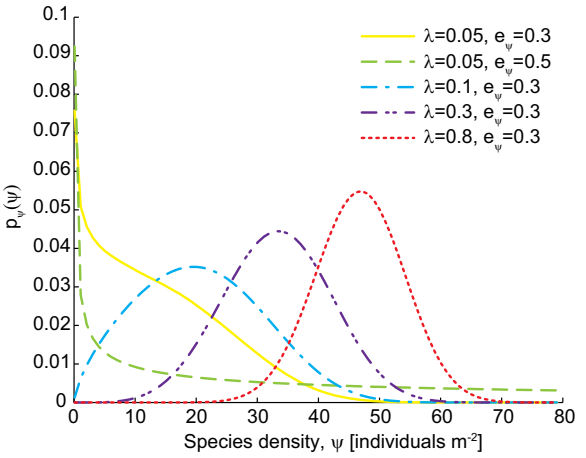

Figure 1. Graphical representation of possible shapes of the analytical pdf of habitat suitability (equation (21)), expressed in terms of species density, for different parameter combinations: $\lambda = 0.05\text{day}^{-1}$, $e_\psi = 0.3$ (yellow solid line), $\lambda = 0.05\text{day}^{-1}$, $e_\psi = 0.5$ (green dashed line), $\lambda = 0.1\text{day}^{-1}$, $e_\psi = 0.3$ (blue dashed-dotted line), $\lambda = 0.3\text{day}^{-1}$, $e_\psi = 0.3$ (violet dashed-double dotted line), and $\lambda = 0.8\text{day}^{-1}$, $e_\psi = 0.3$ (red dotted line). The remaining parameters are: $k = 0.2\text{day}^{-1}$, $\alpha = 0.9\text{mm}$, $A = 100\text{km}^2$, $c_\psi = 0.84\text{m}^{-3e_\psi}\,\text{day}^{e_\psi}$.

3.1. Site Description

The study catchment has a drainage area of 255 km^2, an average elevation of 937 m asl (above sea level) and a maximum elevation of 1892 m asl, while the outlet is located at an elevation of 532 m asl. The catchment is covered by managed spruce and mixed spruce/beech forests (82%) with minor contributions of alpine meadow (11%) and interspersed pastures for cattle and sheep grazing at lower altitudes; bare rock, settlement surfaces, and roads are minimal; the catchment does not have any tilled agricultural surfaces. Geology of the whole catchment is dominated by calcareous, dolomitic limestone with intermittent calcium-poor sandstone and clay shale layers in some subcatchments, higher mountainous areas are karstic. The climate is prealpine with an average annual precipitation of approximately 900 mm and an average temperature of approximately 7.0°C. Monthly average rainfall fluctuates between 40 and 130 mm with strongest rainfall during the summer months from May to September. Precipitation as snow and snow cover are usual from November to April.

3.2. Hydrologic Data

Available daily rainfall measurements have been recorded from 1971 to 2011 in the Biological Station Lunz in Lunz am See. We use daily streamflow data from three gauging stations located within the study catchment (Lunz am See, Seebach, and Goestling, see Figure 2). An additional daily streamflow time series recorded at a nearby location (i.e., Opponitz) located downstream in the study network is also considered in the analysis, as explained in detail below. Discharge data have been collected by the Department of Hydrology and Geoinformation of the Provincial Government of Lower Austria.

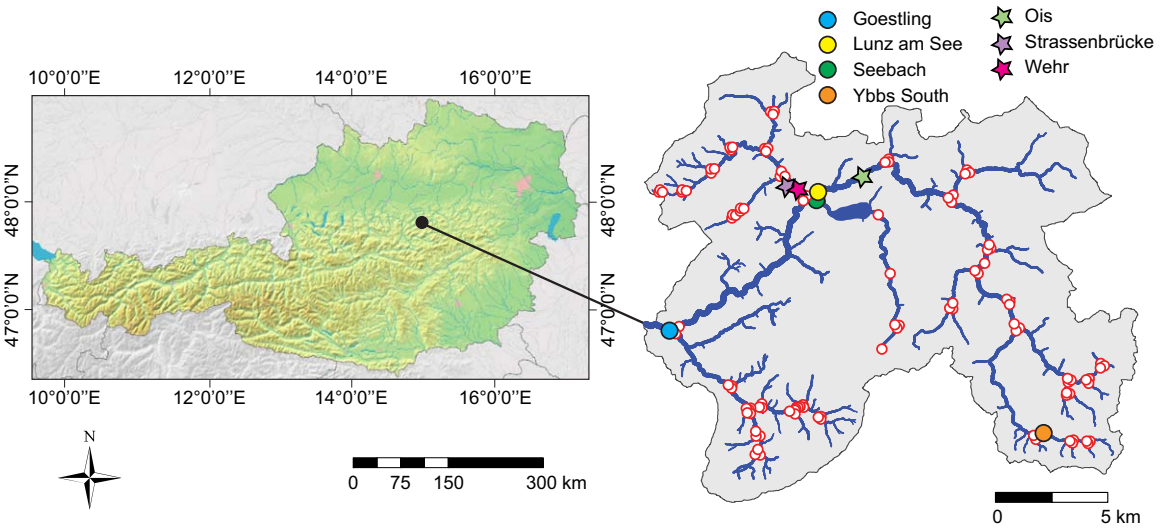

Figure 2. Study catchment: Ybbs River closed at Goestling (Austria) and study sites locations. White dots represent sites whose hydraulic properties are known. The streamflow gauging stations within the catchment are located in Lunz am See (yellow dot), Seebach (green dot), and Goestling (light blue dot). The invertebrate sampling locations are Ybbs upstream Lunz—Ois (light green star), Ybbs downstream Lunz—Strassenbrücke (violet star), and Ybbs downstream Lunz—Wehr (magenta star). The orange dot identifies an additional site (Ybbs South) used for hydrologic analysis.

Table 1. Summary of the Key Geographical and Hydrologic Features of the Streamflow Gauging Stations

Station	Drainage area, A (km^2)	Period	Mean discharge $\langle Q \rangle$ (m^{3}s^{-1})	λ (day^{-1})	k (day^{-1})
Lunz am See	117.9	1984–2010	4.42	0.34	0.24
Goestling	254.1	2009–2010	23.31	0.59	0.45
Seebach	24.8	1997–2010	1.65	0.59	0.22
Opponitz	506.9	1976–2010	19.92	0.35	0.18
Average				*0.53*	

3.3. Invertebrate Density Data

Invertebrate sampling has been conducted using the Surber approach (i.e., a 0.1 m^2 area of the streambed is gently perturbed down to a depth from 5 to 10 cm and all the invertebrates are collected downstream in a net). Mayfly abundance and distribution of *Baetis muticus*, *Baetis rhodani*, and *Ecdyonurus venosus* species are available for three sampling sites: Ybbs upstream Lunz—Ois (Figure 2, light green star), Ybbs downstream Lunz—Strassenbrücke (Figure 2, violet star), and Ybbs downstream Lunz—Wehr (Figure 2, magenta star), where the last two sites are close to each other (nearly 50 m of distance). Note that in what follows, for brevity we will refer to the three sampling sites as Ois, Strassenbrücke, and Wehr.

3.4. Streamflow Probability Distribution Function: Characterization and Parameter Estimation

Given the interannual variability of the hydrologic regime of the study catchment and according to the analytical model assumptions discussed in section 2, a 3 month period with constant rainfall statistics and geomorphological properties is taken into account. In particular, we focus on the summer season (from June to August) here, partly to avoid confounding effects from snow accumulation and snow melt. The mean rainfall depth α and average rainfall frequency λ_p are derived directly from rainfall data, where $\alpha = 9.6$ mm and $\lambda_p = 0.59$ day^{-1}, while the value of λ (i.e., average frequency of streamflow-producing rainfall events) is estimated by means of a mass balance between the mean inflow $\alpha A \lambda$ and the mean outflow $\langle Q \rangle$ at each gauging station (Table 1). The inverse of the mean response time of the catchment k is evaluated from streamflow data, looking at the recession curves corresponding to each of the four gauging stations (Table 1). Given that the streamflow gamma distribution refers to the slow-component of runoff, mainly subsurface runoff, fast-surface runoff components are excluded from the recession analysis for the estimation of k. Following *Botter et al*. [2010], discharge values equaling or exceeding the 90 percentile are disregarded and a linear regression of $-\mathrm{d}Q/\mathrm{d}t$ versus Q [*Botter et al*., 2007a] is performed.

Our analytical streamflow distributions and flow duration curves [*Vogel and Fennessey*, 1994] match reasonably well to the corresponding streamflow statistics derived from the discharge measurements in Lunz am See, Seebach, Goestling (Figure 3), and Opponitz (Figure S1). The streamflow gamma distribution (equation (1)) is able to fairly reproduce the observed probability distribution in Lunz am See and Opponitz, both characterized by reliable estimates of k. In fact, discharge data for these two stations are available for a long period compared to Goestling, whose discharge time series covers two years only. In Goestling, the streamflow analysis leads to an underestimation of the streamflow mode and to a slight overestimation of the probability distribution values between 10 and 50 m^3 s^{-1}, although the shape of the probability distribution is well depicted. In Seebach, as well, the analytical model does not reproduce the peak of the observed streamflow distribution and thus the modeled flow duration curve does not properly match the observed one. This lack of correspondence may be attributable to the position of the gauging station located immediately downstream of Lake Lunz. Therefore, lake dynamics may affect the value of k.

3.5. Basin-Scale Analysis of Streamflow and Bottom Shear Stress Probability Distribution Functions

The Ybbs river network is extracted from a digital elevation model (DEM) of the catchment (10 m pixel size) by (i) computing directions of maximum slope for each pixel, (ii) accumulating the number of upstream located pixels, and (iii) defining a stream when a certain cumulative upstream pixel number threshold was reached. Additional headwater source locations (headwater starts) were manually added based on 1:50.000 topographical maps with hydrological information and ground truthing work. To each stream site i one can associate the total contributing area A_i, i.e., the number of unit areas draining through i following the flow directions defined by the local topographic gradients.

Measurements of stream network hydraulic properties (i.e., stream width w, water depth d, flow velocity v, and discharge Q) were recorded once in 2010 at 124 sites scattered across the considered catchment, and

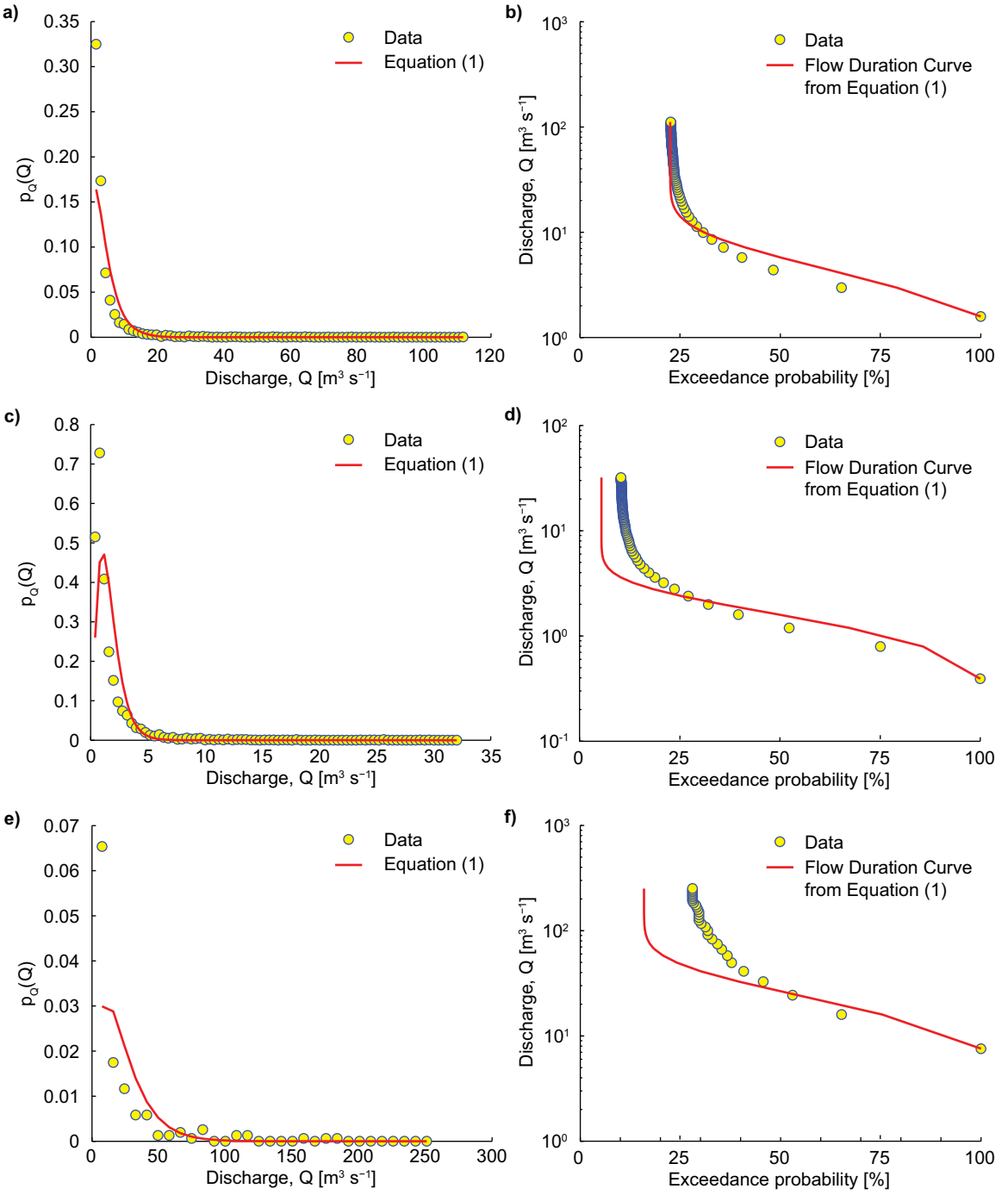

Figure 3. Streamflow statistics: comparison between analytical (red solid line) and observed (circles) streamflow probability distribution functions and flow duration curves in (a and b) Lunz am See, (c and d) Seebach, and (e and f) Goestling.

serve to derive geomorphic scaling relations [*Leopold et al.*, 1964]. The estimated exponent values for stream width, water depth and flow velocity are respectively $e_w = 0.44$, $e_d = 0.27$, and $e_v = 0.29$, quite close to the values found by *Raymond et al.* [2012] (Figure 4). The fitted exponent for bed roughness is $e_n = -0.35$.

Streambed slope is determined from the DEM, as $s_{ij} = \Delta z_{ij} / \Delta l_{ij}$, where s_{ij} is the slope between the sites i and j, Δz_{ij} is the difference in elevation and Δl_{ij} is the distance between the two sites along the drainage direction. A power-law fit of slope values to the corresponding drainage areas provides an exponent of $e_s = -0.50$, which agrees with empirical findings [*Leopold et al.*, 1964]. The scaling relation for the catchment

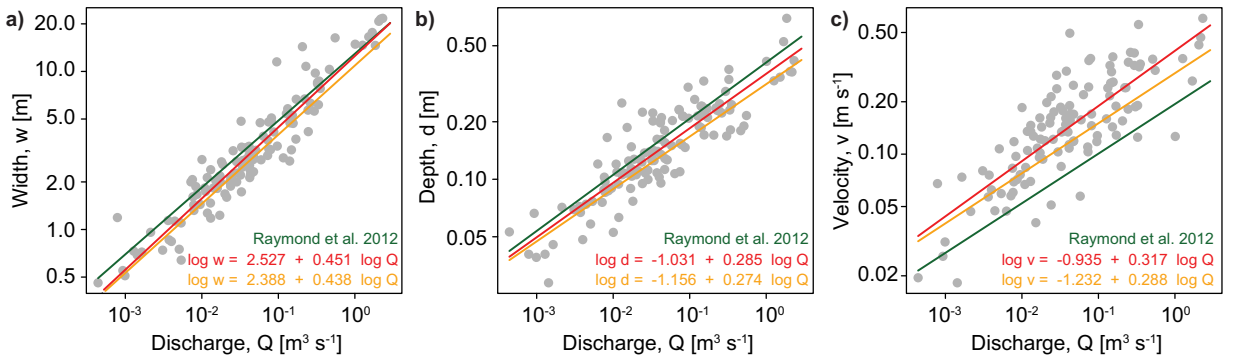

Figure 4. Scaling relations for (a) river width *w*, (b) water depth *d*, and (c) flow velocity *v*. Gray circles represent the hydraulic properties of the 124 sampling sites scattered within the Ybbs catchment. The orange lines show the results of a constrained fitting procedure where we impose that the sum of the exponents is equal to one, while the red lines identify a fitting approach in which *w*, *d*, and *v* are fitted separately. The green lines represent the results obtained by *Raymond et al*. [2012], reported for a comparison.

response time is then derived from the response time values in Lunz am See and Opponitz (i.e., the only two gauging stations providing plausible k values and a remarkably good performance of the streamflow gamma distribution) against respective drainage areas. In this case $e_k = -0.19$, a value slightly above the range suggested by *Pilgrim* [1987] and *Robinson and Sivapalan* [1997].

The spatial variability of streamflow along the Ybbs network is assessed from equations (11) to (13), where α and λ are assumed constant within the catchment (equal to the average estimate of the four gauging stations, Table 1), while k varies according to its scaling relation. $\langle Q \rangle$ spans four orders of magnitude, from 10^{-3} to 10^{1} m^3 s^{-1}, moving upstream to downstream (Figure 5a). For two selected sites of the network differing in drainage area, we computed discharge time series and associated probability distribution functions $p_Q(Q)$ (Figures 5b–5e), as realizations of the modeling of the stochastic process (equation (1)). In these two sites, both the discharge magnitude and the probability distribution present significantly different values. The dispersion of $Q(t)$ with respect to $\langle Q \rangle$ reveals an interesting behavior: low-order stream reaches, located in the upstream part of the basin (Figures 5b and 5c), show a high discharge variability ($CV_Q \simeq 1$), while moving downstream, the deviation from the mean value decreases down to almost 60% (Figures 5d and 5e).

To derive the spatial distribution of bottom shear stress, we assume uniform flow conditions and an equivalent rectangular cross section as reasonable working hypotheses. As the measured river widths in the 124 sites are markedly higher than recorded water depths, the hydraulic radius R_h approximates water depth, which we can thus use to estimate reasonable network-wide bottom shear stress values using its scaling relation with Q (equation (8)).

The spatial distribution of temporal mean shear stress values $\langle \tau \rangle$ is characterized by a decreasing pattern in the downstream direction, mainly controlled by the streambed slope (Figure 6). Lower shear stress values are found in the downstream reaches (Figures 6b and 6c, light blue lines corresponding to Goestling), where the product between water depth and bed slope shows smaller values. The dispersion of $\tau(t)$ around the mean value highlights a pattern with lower and less variable CV_τ values with respect to CV_Q. Upstream channels (e.g., Ybbs South, Figure 6 in orange) present higher shear stress temporal variability with respect to downstream reaches, due to the fact that higher CV_τ values mainly depend on bed slope, which decreases significantly in the downstream direction. This behavior clearly reflects the enhanced discharge temporal fluctuations typical of low-order reaches, which are primarily associated to a short catchment response time.

3.6. Basin-Scale Analysis of Invertebrate Habitat Suitability to Shear Stress

From the spatial distribution of bottom shear stress along the Ybbs river network, a first-order ecological extension is performed, aiming at the characterization of spatially explicit probability distribution functions of benthic invertebrate habitat suitability to shear stress. Invertebrate habitat suitability curves derived from a prealpine stream and expressed in terms of species density (i.e., normalized to the maximum observed areal abundance) as a function of shear stress [*Schmedtje*, 1995] are employed here. Suitability values thus lie between 0 and 1, where $\psi = 0$ represents the habitat state characterized by the absence of invertebrates

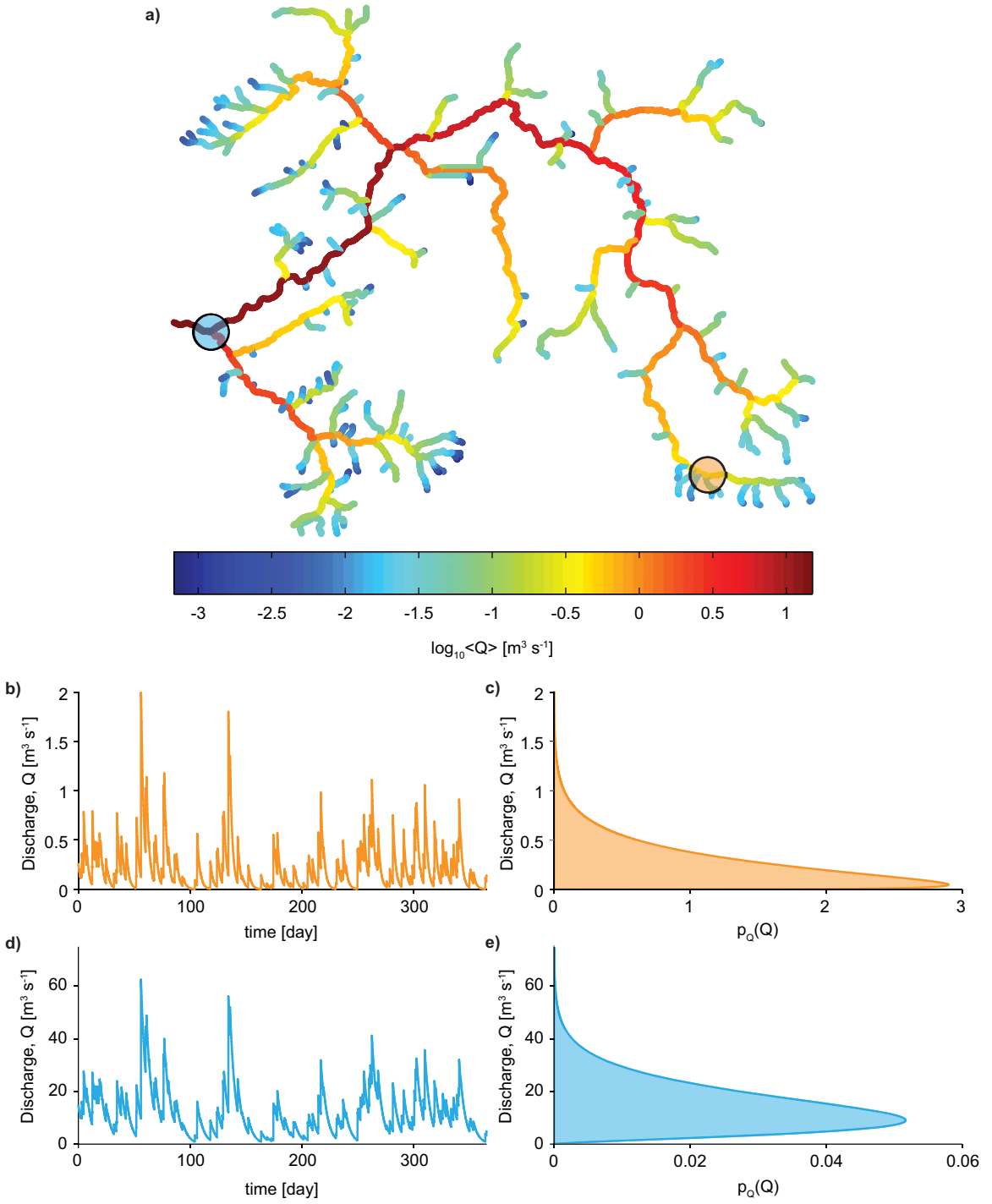

Figure 5. Discharge variability along the Ybbs river network as realizations of the modeling of a stochastic process (equation (1)): (a) $\langle Q \rangle$, (b and d) time series, and (c and e) probability distribution functions for the locations Goestling (light blue) and Ybbs South (orange).

and $\psi = 1$ corresponds to the maximum species density condition. In accordance with the hydrological analysis, the summer generations of three mayfly species, namely *Baetis muticus*, *Baetis rhodani*, and *Ecdyonurus venosus*, are considered. Recalling equation (19), which defines an analytical relation between habitat suitability and bottom shear stress, a power-law fit is performed in order to estimate the values of c_{ψ_τ}, e_{ψ_τ}, c_ψ, and e_ψ (see Table 2). *Baetis muticus* and *Ecdyonurus venosus* habitat suitability curves for the summer generation show a monotonically decreasing trend of normalized individual densities with increasing bottom

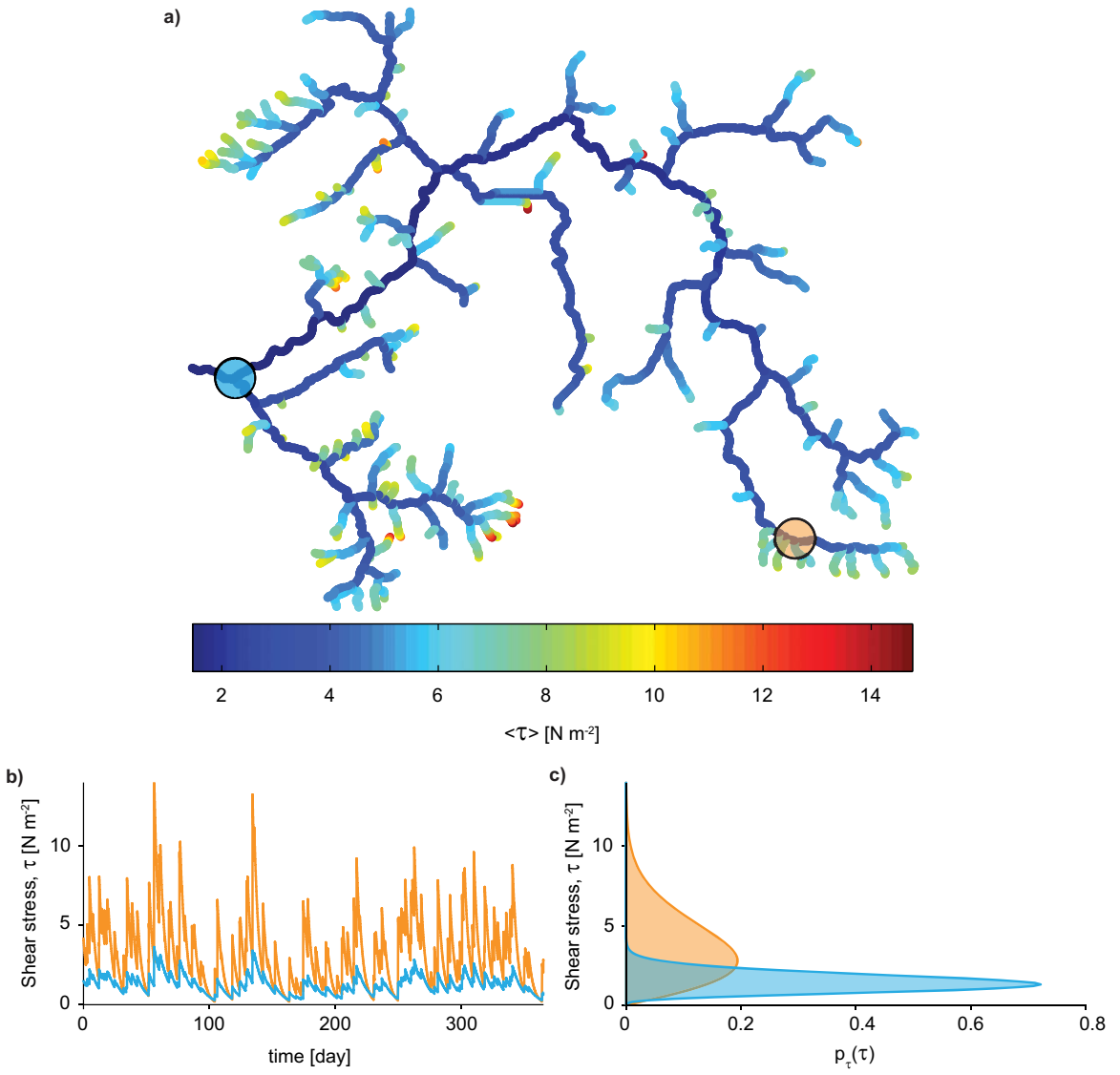

Figure 6. Bottom shear stress variability along the Ybbs river network as realizations of the modeling of a stochastic process (equation (4)): (a) $\langle\tau\rangle$, (b) time series, and (c) probability distribution functions for the locations Goestling (light blue) and Ybbs South (orange).

shear stress, thus revealing in principle a preference for downstream reaches, characterized by relatively small shear stress values if compared to low-order branches (Table 2 and Figure 7). Conversely, *Baetis rhodani* presents a positive exponent of the power-law relation (equation (19) and Table 2), which results in a decreasing downstream suitability to shear stress. Average suitabilities $\langle\psi\rangle$ along the Ybbs river network, exclusively influenced by near-bed flow conditions, are estimated from equation (21) for each of the considered mayfly species (see Figure 7). The performed analysis postulates average suitabilities to near-bed flow conditions of *Baetis muticus* sp. (Figure 7a) ranging from nearly $\langle\psi\rangle=0.6$ in the low-order reaches to almost $\langle\psi\rangle=1$ approaching the outlet. The spatial variability of *Ecdyonurus venosus* (Figure 7c) average habitat suitability to shear stress along the Ybbs river network shows a trend similar to *Baetis muticus*, although with considerable smaller values (ranging from $\langle\psi\rangle=0.2$ to $\langle\psi\rangle=0.4$). The model results for *Baetis rhodani* suggest a decline in habitat suitability moving in the downstream direction, from

Table 2. Invertebrate Habitat Suitability Curves: Estimated Coefficients for Power-Law Equations (19) and (20)

Mayfly Species	c_{ψ_τ} ($kg^{-e_{\psi_\tau}} m^{e_{\psi_\tau}} s^{2e_{\psi_\tau}}$)	e_{ψ_τ} (-)	e_{ψ} (-)
Baetis muticus	1.03	−0.39	−0.23
Baetis rhodani	0.75	0.17	0.10
Ecdyonurus venosus	0.41	−0.41	−0.25

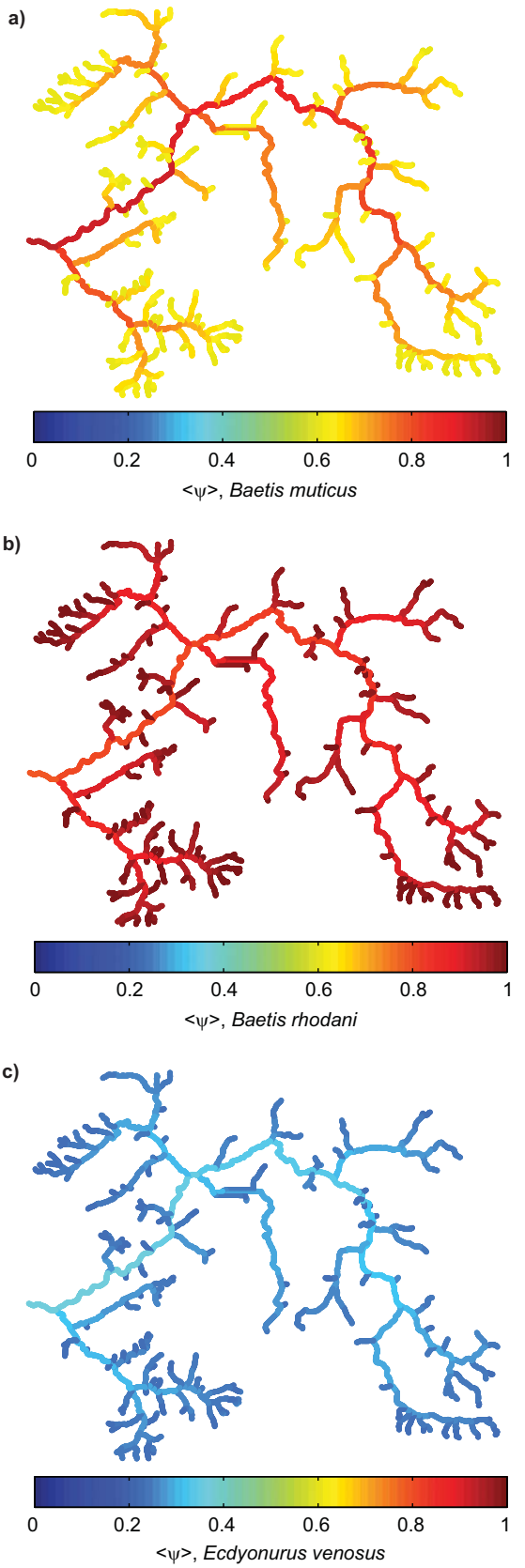

Figure 7. Average habitat suitability based on shear stress along the Ybbs river network as derived from equation (21) for the mayfly species (a) *Baetis muticus*, (b) *Baetis rhodani*, and (c) *Ecdyonurus venosus*.

nearly $\langle\psi\rangle=1$ in correspondence to headwaters to $\langle\psi\rangle=0.7$ in downstream sites (Figure 7b). When comparing the modeled habitat suitabilities for the three mayfly species, the analysis highlights higher $\langle\psi\rangle$ values for *Baetis rhodani* and *Baetis muticus*. Therefore, near-bed flow conditions along the Ybbs river network seem to be more favorable for these two mayfly species, whereas *Ecdyonurus venosus* seems to prefer lower shear stress.

4. Discussion

The analytical approach developed in this paper aims at the estimation of benthic invertebrate habitat suitability with reference to shear stress in a fluvial network. Shear stress is considered here as an adequate descriptor of near-bed flow conditions, and thus regarded as the prime driver of invertebrate abundance and distribution. We do acknowledge that this approach is simplistic and therefore may have its limitations. In fact, a plethora of additional factors may control invertebrate abundance and distribution. Chief among them is flow history but also ice cover during the winter preceding sampling, local resource availability and predation [*Power et al.*, 1995b; *Poff et al.*, 1997; *Milner et al.*, 2011; *Post et al.*, 2013]. Rather than generating a comprehensive model capturing as many controls on invertebrate distribution as possible, we decide to focus on shear stress as one key physical parameter directly associated to discharge. This simple and practical approach sets the basis to quickly locate priorities for policy development in river basins restoration. The proposed model allows one to identify critical river reaches as well as the ideal river flow regime for the recovery of benthic invertebrate habitats.

To test the model performances, a large set of field data of invertebrate density should be compared with the estimated habitat suitability. A large sample investigation is needed to average out the effects of field data uncertainty and the variability in habitat suitability originated by the above forcings that are not considered by the model. A first model testing experiment is herein presented, based on a field campaign during which the abundance of three different

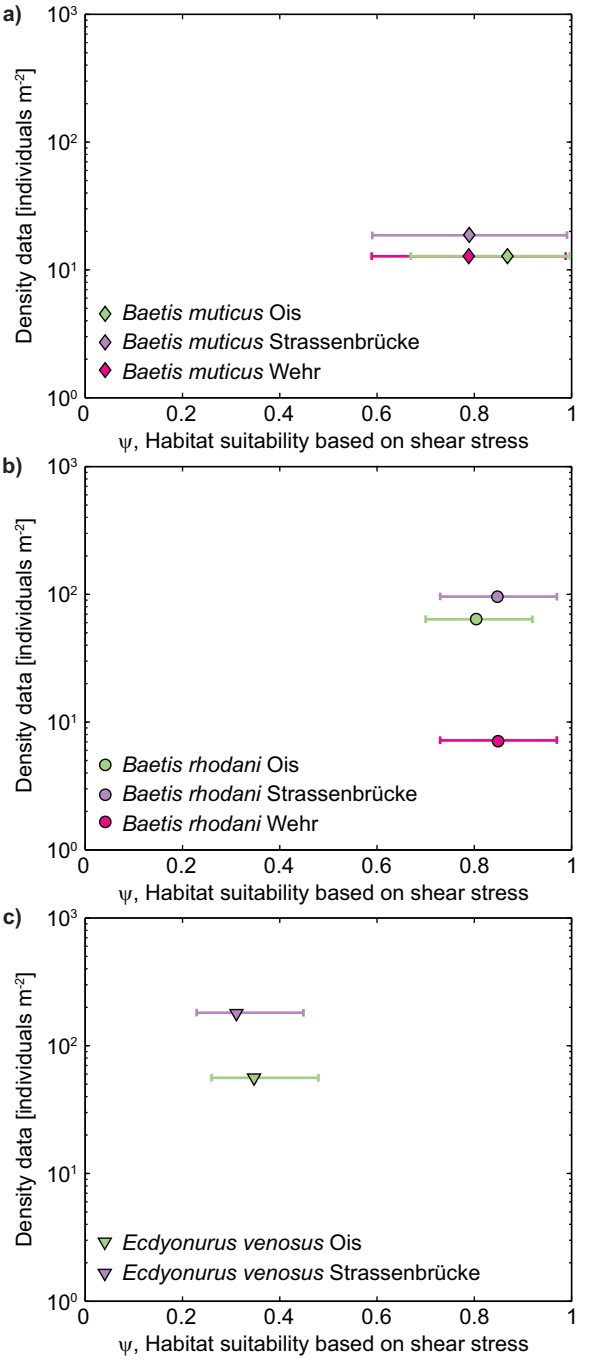

Figure 8. Comparison of individual invertebrate density data against the analytical habitat suitability to shear stress ($\langle\psi\rangle$ and 5–95 percentiles) evaluated from equation (21) in correspondence to the sampling sites of Ybbs upstream Lunz—Ois (light green), Ybbs downstream Lunz—Strassenbrücke (violet), and Ybbs downstream Lunz—Wehr (magenta) for the mayfly species (a) *Baetis muticus*, (b) *Baetis rhodani*, and (c) *Ecdyonurus venosus*.

mayfly species was measured in three river sections. One would expect that, for the same species in different locations, an increasing invertebrate abundance is associated to increasing habitat suitability. The results are presented in Figure 8, where observed invertebrate abundances are displayed against predictions of habitat suitability with regard to shear stress ($\langle\psi\rangle$, and 5–95 percentiles), as derived from equation (21) and previously shown in Figure 7. The results reveal that the limited sample size of the field data and the proximity of the river sections located at Strassenbrücke and Wehr do not allow one to obtain a clear conclusion on the modeled patterns. However, interesting findings emerge for *Baetis rhodani* (Figure 8b), where the estimated suitability seems to match the progress of invertebrate abundance. A more extended spatiotemporal invertebrate sampling campaign, including upstream reaches and sites close to the outlet and spanning over several years, would be needed to obtain a reliable test of model performances. Nevertheless, we believe that the presented comparison proves reasonable model results, not completely inconsistent with respect to field data.

In addition, the proposed approach, moving from the spatiotemporal pattern of hydrologic conditions along the Ybbs river network, considers the whole range of discharge $Q(t)$ and shear stress $\tau(t)$ temporal sequences to evaluate the temporal trend of $\psi(t)$ and thus its temporal average $\langle\psi\rangle$. An oversimplification, where $\langle\psi\rangle$ values are estimated by simply considering $\langle Q\rangle$ and $\langle\tau\rangle$, produces markedly different results. Indeed, hydrologic fluctuations critically control invertebrate habitat suitability (Figure 9). Average suitabilities with regard to shear stress $\langle\psi\rangle$ calculated from either $Q(t)$ (red solid line) or $\langle Q\rangle$ (green dashed line) are consistently different, due to the nonlinearity of the habitat suitability-discharge relationship (equation (20)).

The present study moves the typical reach-level observations of benthic community ecology to the level of entire stream networks. This is crucial for several reasons. First, it could pave the way for conservation

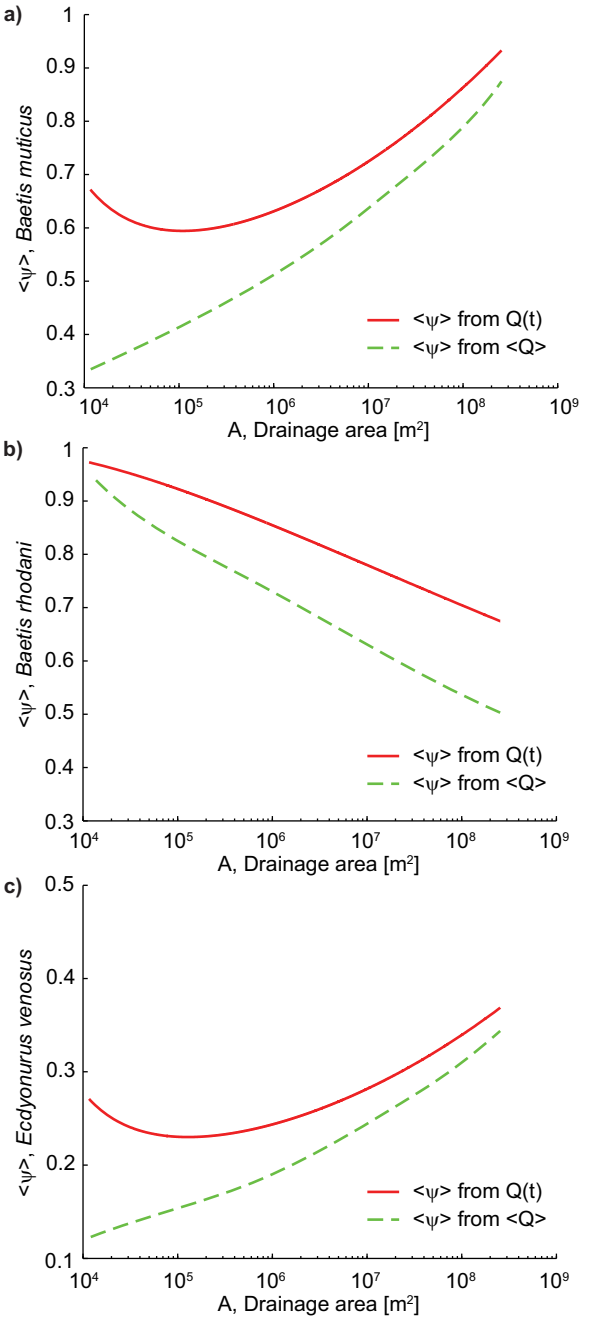

Figure 9. Comparison of average habitat suitability based on shear stress $\langle\psi\rangle$ versus drainage area calculated from $Q(t)$ (red solid line) and $\langle Q\rangle$ (green dashed line) for the mayfly species (a) *Baetis muticus*, (b) *Baetis rhodani*, and (c) *Ecdyonurus venosus*.

strategies based on metacommunity ecology in a dendritic landscape, such as a fluvial networks [*Economo*, 2011; *Montoya et al*., 2012]. Given the often large scale of anthropogenic disturbance, it is in fact crucial to move beyond the scale of an individual reach. Second, current shifts in hydrological regime at the level of fluvial networks due to interbasin water transfer and damming, for instance, affect biodiversity patterns [e.g., *Campbell Grant et al*., 2012]. Predicted shifts in the hydrological regime due to climate change [*IPCC*, 2013] may hasten the perturbation of biodiversity patterns at the scale of fluvial network. Therefore, our model offers a valuable theoretical framework to assess such changes for benthic invertebrate biodiversity and its possible reshuffling at landscape scale.

5. Conclusions

In this paper, we perform an ecological extension of hydrologic tools, i.e., streamflow probability distributions and associated flow duration curves, to a prealpine stream network. In particular, we use hydrologic conditions and the river network structure to predict shear stress as a major determinant of invertebrate habitat suitability throughout the stream network. Our approach essentially follows two steps:

1. First, the spatiotemporal variability of discharge and associated bottom shear stress along a river network is analyzed. Based on site-specific probability distribution functions, we achieve a spatial extension through suitable scaling relations expressed as a function of either discharge or drainage area. In the same manner, spatially explicit probability distribution functions for any other hydrologic variable showing a spatial variation across a stream network could be derived. These analytical tools are applied to the Ybbs catchment, located in Austria, where rainfall and streamflow time series and river network hydraulic characteristics are available.

2. In a second step, we compute habitat suitability curves, i.e., proximate expressions of species density as a function of bottom shear stress, for three mayfly species from published data, and analytically characterize their probability distribution functions. The effects of the river network spatial organization and of the hydrologic features on habitat suitability are then examined using habitat suitability probability distribution

maps. By means of the analytical tool here derived, we are able to assess average invertebrate habitat suitability based on one ecological major determinant, i.e., shear stress, as a function of key hydrologic, geomorphologic, and meteorologic properties. Our model predictions are compared against observed invertebrate densities in three locations within the examined catchment. Although based on a very limited sample size, this preliminary analysis shows that the model predictions provide a reasonable interpretation of field data. Our results clearly emphasize that more sampling experiments, with possibly very different drainage areas, are nevertheless needed to extensively test model performances. Our proposed approach is a valuable tool for the management of water resources, e.g., for the proper definition of streamflow requirements, and lends itself to a number of important spinoffs, notably in the fields that include stream primary production, food-web length, habitat suitability and organization, and eventually large scale carbon fluxes. Habitat suitability maps may help to guide habitat protection and to assess the ecological integrity of a stream network or parts thereof. The latter can be achieved by taking into account anthropogenically induced changes to streamflow, e.g., as occurring by damming and streamflow diversions. Here our approach could be used to indicate hotspots of anthropogenic influence by comparing observed patterns of human-altered streamflows to modeling results expressing the expected pattern for a natural flow regime.

Acknowledgments

S.C., E.B., and A.R. gratefully acknowledge the support provided by ERC advanced grant program through the project RINEC-227612 and by the SFN/FNS projects 200021_124930 and 200020_140661. S.C. and A.M. acknowledge the financial support from the EU funded project SWITCH-ON-603587. T.J.B. acknowledges financial support from FWF (START Y420-B17). We further thank Christian Krammer from the Department of Hydrology and Geoinformation of the Provincial Government of Lower Austria for provision of discharge time series.

References

Allan, J., and M. Castillo (2007), *Stream Ecology: Structure and Function of Running Waters*, Springer, Dordrecht, Netherlands.

Armanini, A. (1995), Nonuniform sediment transport—Dynamics of the active layer, *J. Hydraul. Res.*, *33*(5), 611–622.

Armanini, A., and G. Di Silvio (1988), A one-dimensional model for the transport of a sediment mixture in non-equilibrium conditions, *J. Hydraul. Res.*, *26*(3), 275–292.

Banavar, J., A. Maritan, and A. Rinaldo (1999), Size and form in efficient transportation networks, *Nature*, *399*(6732), 130–132, doi:10.1038/20144.

Battin, T., L. Kaplan, S. Findlay, C. Hopkinson, E. Marti, A. Packman, J. Newbold, and F. Sabater (2008), Biophysical controls on organic carbon fluxes in fluvial networks, *Nat. Geosci.*, *1*(2), 95–100, doi:10.1038/ngeo101.

Bertuzzo, E., R. Muneepeerakul, H. Lynch, W. Fagan, I. Rodriguez-Iturbe, and A. Rinaldo (2009), On the geographic range of freshwater fish in river basins, *Water Resour. Res.*, *45*, W11420, doi:10.1029/2009WR007997.

Bertuzzo, E., S. Suweis, L. Mari, A. Maritan, I. Rodriguez-Iturbe, and A. Rinaldo (2011), Spatial effects on species persistence and implications for biodiversity, *Proc. Natl. Acad. Sci. U. S. A.*, *108*(11), 4346–4351, doi:10.1073/pnas.1017274108.

Besemer, K., G. Singer, C. Quince, E. Bertuzzo, W. Sloan, and T. Battin (2013), Headwaters are critical reservoirs of microbial diversity for fluvial networks, *Proc. R. Soc. B*, *280*(1771), 20131760, doi:10.1098/rspb.2013.1760.

Beven, K. (2001), *Rainfall-Runoff Modelling: The Primer*, Wiley, Chichester.

Biggs, B., M. Duncan, I. Jowett, J. Quinn, C. Hickey, R. Daviescolley, and M. Close (1990), Ecological characterization, classification, and modeling of New-Zealand rivers—An introduction and synthesis, *N. Z. J. Mar. Freshwater Res.*, *24*(3), 277–304.

Booker, D., T. Snelder, M. Greenwood, and S. Crow (2014), Relationships between invertebrate communities and both hydrological regime and other environmental factors across New Zealand's rivers, *Ecohydrology*, doi:10.1002/eco.1481.

Botter, G., A. Porporato, I. Rodriguez-Iturbe, and A. Rinaldo (2007a), Basin-scale soil moisture dynamics and the probabilistic characterization of carrier hydrologic flows: Slow, leaching-prone components of the hydrologic response, *Water Resour. Res.*, *43*, W02417, doi:10.1029/2006WR005043.

Botter, G., F. Peratoner, A. Porporato, I. Rodriguez-Iturbe, and A. Rinaldo (2007b), Signatures of large-scale soil moisture dynamics on streamflow statistics across US climate regimes, *Water Resour. Res.*, *43*, W11413, doi:10.1029/2007WR006162.

Botter, G., S. Zanardo, A. Porporato, I. Rodriguez-Iturbe, and A. Rinaldo (2008), Ecohydrological model of flow duration curves and annual minima, *Water Resour. Res.*, *44*, W08418, doi:10.1029/2008WR006814.

Botter, G., S. Basso, A. Porporato, I. Rodriguez-Iturbe, and A. Rinaldo (2010), Natural streamflow regime alterations: Damming of the Piave river basin (Italy), *Water Resour. Res.*, *46*, W06522, doi:10.1029/2009WR008523.

Brutsaert, W. (2005), *Hydrology: An Introduction*, Cambridge Univ. Press, New York.

Campbell Grant, E., W. Lowe, and W. Fagan (2007), Living in the branches: Population dynamics and ecological processes in dendritic networks, *Ecol. Lett.*, *10*, 165–175.

Campbell Grant, E., H. Lynch, R. Muneepeerakul, M. Arunachalam, I. Rodriguez-Iturbe, and W. Fagan (2012), Interbasin water transfer, riverine connectivity, and spatial controls on fish biodiversity, *PLoS ONE*, *7*(3), e34170, doi:10.1371/journal.pone.0034170.

Carrara, F., F. Altermatt, I. Rodriguez-Iturbe, and A. Rinaldo (2012), Dendritic connectivity controls biodiversity patterns in experimental metacommunities, *Proc. Natl. Acad. Sci. U. S. A.*, *109*(15), 5761–5766, doi:10.1073/pnas.1119651109.

Ceola, S., G. Botter, E. Bertuzzo, A. Porporato, I. Rodriguez-Iturbe, and A. Rinaldo (2010), Comparative study of ecohydrological streamflow probability distributions, *Water Resour. Res.*, *46*, W09502, doi:10.1029/2010WR009102.

Ceola, S., I. Hoedl, M. Adlboller, G. Singer, E. Bertuzzo, L. Mari, G. Botter, J. Waringer, T. Battin, and A. Rinaldo (2013), Hydrologic variability affects invertebrate grazing on phototrophic biofilms in stream microcosms, *PLoS ONE*, *8*(4), e60629, doi:10.1371/journal.pone.0060629.

Chow, V. (1964), *Handbook of Applied Hydrology*, McGraw-Hill, New York.

Chow, V., D. Maidment, and L. Mays (1988), *Applied Hydrology*, McGraw-Hill, New York.

Doledec, S., N. Lamouroux, U. Fuchs, and S. Merigoux (2007), Modelling the hydraulic preferences of benthic macroinvertebrates in small European streams, *Freshwater Biol.*, *52*(1), 145–164, doi:10.1111/j.1365-2427.2006.01663.x.

Economo, E. (2011), Biodiversity conservation in metacommunity networks: Linking pattern and persistence, *Am. Nat.*, *177*(6), E167–E180, doi:10.1086/659946.

Fagan, W. (2002), Connectivity, fragmentation, and extinction risk in dendritic metapopulations, *Ecology*, *83*, 3243–3249.

Gore, J., J. Layzer, and J. Mead (2001), Macroinvertebrate instream flow studies after 20 years: A role in stream management and restoration, *Regul. Rivers Res. Manage.*, *17*(4–5), 527–542, doi:10.1002/rrr.650.abs.
Hart, D., and C. Finelli (1999), Physical-biological coupling in streams: The pervasive effects of flow on benthic organisms, *Ann. Rev. Ecol. Syst.*, *30*, 363–395, doi:10.1146/annurev.ecolsys.30.1.363.
IPCC (2013), *Climate Change 2013: The Physical Science Basis. Contribution of Working Group I to the Fifth Assessment Report of the Intergovernmental Panel on Climate Change*, Cambridge Univ. Press, Cambridge, U. K.
Johnson, N., S. Kotz, and N. Balakrishnan (1994), *Continuous Univariate Distributions*, vol. *1*, John Wiley, New York.
Jowett, I., and J. Richardson (1990), Microhabitat preferences of benthic invertebrates in a New Zealand river and the development of instream flow-habitat models for *Deleatidium* spp., *N. Z. J. Mar. Freshwater Res.*, *24*(1), 19–30.
Jowett, I., J. Richardson, B. Biggs, C. Hickey, and J. Quinn (1991), Microhabitat preferences of benthic invertebrates and the development of generalized *Deleatidium* spp. habitat suitability curves, applied to 4 New-Zealand rivers, *N. Z. J. Mar. Freshwater Res.*, *25*(2), 187–199.
Lamouroux, N., S. Merigoux, S. Doledec, and T. Snelder (2013), Transferability of hydraulic preference models for aquatic macroinvertebrates, *River Res. Appl.*, *29*(7), 933–937, doi:10.1002/rra.2578.
Lancaster, J., and A. Hildrew (1993), Flow refugia and the microdistribution of lotic macroinvertebrates, *J. N. Am. Benthol. Soc.*, *12*(4), 385–393, doi:10.2307/1467619.
Lancaster, J., T. Buffin-Belanger, I. Reid, and S. Rice (2006), Flow- and substratum-mediated movement by a stream insect, *Freshwater Biol.*, *51*(6), 1053–1069, doi:10.1111/j.1365-2427.2006.01554.x.
Leopold, L., M. Wolman, and J. Miller (1964), *Fluvial Processes in Geomorphology*, W. H. Freeman, San Francisco, Calif.
Malmqvist, B., and G. Sackmann (1996), Changing risk of predation for a filter-feeding insect along a current velocity gradient, *Oecologia*, *108*(3), 450–458, doi:10.1007/BF00333721.
Mejía, A., E. Daly, F. Rossel, T. Jovanovic, and J. Gironás (2014), A stochastic model of streamflow for urbanized basins, *Water Resour. Res.*, *50*, doi:10.1002/2013WR014834.
Merigoux, S., N. Lamouroux, J. Olivier, and S. Doledec (2009), Invertebrate hydraulic preferences and predicted impacts of changes in discharge in a large river, *Freshwater Biol.*, *54*(6), 1343–1356, doi:10.1111/j.1365-2427.2008.02160.x.
Merritt, R., and K. Cummins (1996), *An Introduction to the Aquatic Insects of North America*, Kendall/Hunt Publ. Co., Dubuque, Ia.
Milner, A., A. Robertson, L. Brown, S. Sonderland, M. McDermott, and A. Veal (2011), Evolution of a stream ecosystem in recently deglaciated terrain, *Ecology*, *92*(10), 1924–1935.
Montoya, D., L. Rogers, and J. Memmott (2012), Emerging perspectives in the restoration of biodiversity-based ecosystem services, *Trends Ecol. Evol.*, *27*(12), 666–672, doi:10.1016/j.tree.2012.07.004.
Muneepeerakul, R., J. Weitz, S. Levin, A. Rinaldo, and I. Rodriguez-Iturbe (2007), A neutral metapopulation model of biodiversity in river networks, *J. Theor. Biol.*, *245*(2), 351–363, doi:10.1016/j.jtbi.2006.10.005.
Muneepeerakul, R., E. Bertuzzo, H. Lynch, W. Fagan, A. Rinaldo, and I. Rodriguez-Iturbe (2008), Neutral metacommunity models predict fish diversity patterns in Mississippi-Missouri basin, *Nature*, *453*(7192), 220–222, doi:10.1038/nature06813.
Orlandini, S., and R. Rosso (1998), Parameterization of stream channel geometry in the distributed modeling of catchment dynamics, *Water Resour. Res.*, *34*(8), 1971–1985, doi:10.1029/98WR00257.
Pilgrim, D. E. (1987), *Australian Rainfall and Runoff: A Guide to Flood Estimation*, Inst. of Eng., Barton, ACT, Australia.
Poff, N., and J. Ward (1989), Implications of streamflow variability and predictability for lotic community structure—A regional-analysis of streamflow patterns, *Can. J. Fish. Aquat. Sci.*, *46*(10), 1805–1818, doi:10.1139/f89-228.
Poff, N., and J. Ward (1992), Heterogeneous currents and algal resources mediate in situ foraging activity of a mobile stream grazer, *Oikos*, *65*(3), 465–478, doi:10.2307/3545564.
Poff, N., J. Allan, M. Bain, J. Karr, K. Prestegaard, B. Richter, R. Sparks, and J. Stromberg (1997), The natural flow regime, *Bioscience*, *47*(11), 769–784, doi:10.2307/1313099.
Post, E., U. Bhatt, C. Bitz, J. Brodie, T. Fulton, M. Hebblewhite, J. Kerby, S. Kutz, I. Stirling, and D. Walker (2013), Ecological consequences of sea-ice decline, *Science*, *341*(6145), 519–524, doi:10.1126/science.1235225.
Power, M., G. Parker, W. Dietrich, and A. Sun (1995a), How does floodplain width affect river ecology—A preliminary exploration using simulations, *Geomorphology*, *13*(1–4), 301–317, doi:10.1016/0169-555X(95)00039-80.
Power, M., A. Sun, G. Parker, W. Dietrich, and J. Wootton (1995b), Hydraulic food-chain models, *Bioscience*, *45*(3), 159–167, doi:10.2307/1312555.
Raymond, P., C. Zappa, D. Butman, T. Bott, J. Potter, P. Mulholland, A. Laursen, W. McDowell, and D. Newbold (2012), Scaling the gas transfer velocity and hydraulic geometry in streams and small rivers, *Limnol. Oceanogr., 2*, 41–53, doi:10.1215/21573689-1597669.
Rinaldo, A., A. Marani, and R. Rigon (1991), Geomorphological dispersion, *Water Resour. Res.*, *27*(4), 513–525, doi:10.1029/90WR02501.
Rinaldo, A., W. Dietrich, R. Rigon, G. Vogel, and I. Rodriguez-Iturbe (1995), Geomorphological signatures of varying climate, *Nature*, *374*(6523), 632–635, doi:10.1038/374632a0.
Robinson, J., and M. Sivapalan (1997), Temporal scales and hydrological regimes: Implications for flood frequency scaling, *Water Resour. Res.*, *33*(12), 2981–2999, doi:10.1029/97WR01964.
Rodriguez-Iturbe, I. (2000), Ecohydrology: A hydrologic perspective of climate-soil-vegetation dynamics, *Water Resour. Res.*, *36*(1), 3–9, doi:10.1029/1999WR900210.
Rodriguez-Iturbe, I., and A. Porporato (2004), *Ecohydrology of Water Controlled Ecosystems: Soil Moisture and Plant Dynamics*, Cambridge Univ. Press, New York.
Rodriguez-Iturbe, I., and A. Rinaldo (1997), *Fractal River Basins: Chance and Self-Organization*, Cambridge Univ. Press, New York.
Rodriguez-Iturbe, I., A. Porporato, L. Ridolfi, V. Isham, and D. Cox (1999), Probabilistic modelling of water balance at a point: The role of climate, soil and vegetation, *Proc. R. Soc. A*, *455*(1990), 3789–3805.
Rodriguez-Iturbe, I., R. Muneepeerakul, E. Bertuzzo, S. Levin, and A. Rinaldo (2009), River networks as ecological corridors: A complex systems perspective for integrating hydrologic, geomorphologic, and ecologic dynamics, *Water Resour. Res.*, *45*, W01413, doi:10.1029/2008WR007124.
Rouget, M., R. Cowling, A. Lombard, A. Knight, and G. Kerley (2006), Designing large-scale conservation corridors for pattern and process, *Conserv. Biol.*, *20*, 549–561, doi:0.1111/j.1523-1739.2006.00297.x.
Schmedtje, U. (1995), Beziehungen zwischen der sohlnahen Strömung, dem Gewässerbett und dem Makrozoobenthos in Fliessgewässern—Ökologische Grundlagen für die Beurteilung von Ausleitstrecken, PhD thesis, Univ. of Innsbruck, Innsbruck, Austria.
Stacy, E. (1962), A generalization of the Gamma distribution, *Ann. Math. Stat.*, *33*(3), 1187–1192.
Statzner, B., and R. Muller (1989), Standard hemispheres as indicators of flow characteristics in lotic benthos research, *Freshwater Biol.*, *21*(3), 445–459, doi:10.1111/j.1365-2427.1989.tb01377.x.

Szemis, J., G. Dandy, and H. Maier (2013), A multiobjective ant colony optimization approach for scheduling environmental flow management alternatives with application to the River Murray, Australia, *Water Resour. Res.*, *49*, 6393–6411, doi:10.1002/wrcr.20518.

Trent, M., and J. Ackerman (2011), Microdistribution of a torrential stream invertebrate: Are bottom-up, top-down, or hydrodynamic controls most important?, *Limnol. Oceanogr.*, *1*, 147–162, doi:10.1215/21573698-1498042.

Vogel, R., and N. Fennessey (1994), Flow-duration curves. 1: New interpretation and confidence-intervals, *J. Water Resour. Plann. Manage.*, *120*(4), 485–504, doi:10.1061/(ASCE)0733-9496(1994)120:4(485).

Vogel, S. (1994), *Life in Moving Fluids*, 2nd ed., Princeton Univ. Press, Princeton, N. J.

Wellnitz, T., N. Poff, G. Cosyleon, and B. Steury (2001), Current velocity and spatial scale as determinants of the distribution and abundance of two rheophilic herbivorous insects, *Landscape Ecol.*, *16*(2), 111–120, doi:10.1023/A:1011114414898.

Zalewski, M., G. Janauer, and G. Jolankai (1997), Ecohydrology: A new paradigm for the sustainable use of aquatic resources, *IHP-V Tech. Doc. in Hydrol. 7*, UNESCO, Paris.